Volume 38 Number 2 February 2011 ISSN 0735-1933

International Communications in Heat and Mass Transfer 38 (2011) 263–274

Contents lists available at ScienceDirect

International Communications in Heat and Mass Transfer

journal homepage: www.elsevier.com/locate/ichmt

Mixed convection heat transfer in a differentially heated square enclosure with a conductive rotating circular cylinder at different vertical locations ☆

Salam Hadi Hussain, Ahmed Kadhim Hussein *

Mechanical Engineering Department, College of Engineering, Babylon University, Babylon Province, Iraq

ARTICLE INFO

Available online 18 December 2010

Keywords:
Mixed convection
Rotating circular cylinder
Enclosure
Conduction
Vertical cylinder locations
Finite volume

ABSTRACT

In this investigation, a numerical simulation using a finite volume scheme is carried out for a laminar steady mixed convection problem in a two-dimensional square enclosure of width and height (L), with a rotating circular cylinder of radius ($R=0.2$ L) enclosed inside it. The solution is performed to analyze mixed convection in this enclosure where the left side wall is subjected to an isothermal temperature higher than the opposite right side wall. The upper and lower enclosure walls are considered adiabatic. The enclosure under study is filled with air with Prandtl number is taken as 0.71. Fluid flow and thermal fields and the average Nusselt number are presented for the Richardson numbers ranging as 0, 1, 5 and 10, while Reynolds number ranging as 50, 100, 200 and 300. The effects of various locations and solid–fluid thermal conductivity ratios on the heat transport process are studied in the present work. The results of the present investigation explain that increase in the Richardson and Reynolds numbers has a significant role on the flow and temperature fields and the rotating cylinder locations have an important effect in enhancing convection heat transfer in the square enclosure. The results explain also, that the average Nusselt number value increases as the Reynolds and Richardson numbers increase and the convection phenomenon is strongly affected by these parameters. The results showed a good agreement with further published works.

1. Introduction

Steady state convection heat transfer from a rotating cylinder to its surrounding enclosure is a subject of practical importance. This type of thermally driven flow is encountered in numerous applications especially in some building service situations, when a pipe carrying a hot water passes through an enclosure formed by structural components of the building, rotating-tube heat exchangers, and the drilling of oil wells. The function of the outer surface of the enclosure is to reduce the heat transfer from the inner rotating hot cylinder or to save the inner body in harsh outdoor environment. In recent years, the flow around a rotating circular cylinder is considered a fundamental fluid mechanics problem of great interest. It has potential relevance to a huge number of practical applications such as submarines, off shore structures, pipelines etc. Several numerical and experimental methods have been developed to investigate enclosures with and without rotating or stationary obstacle because these geometries have great practical engineering applications. Chang et al. [1] made a numerical analysis for natural convective heat transfer in an irregular two-dimensional enclosure formed by an inner square cylinder and an outer circular envelope. They also performed an experimental investigation to verify some of the numerical results. Glapke and Afsaw [2] presented some results for natural convection in a circular enclosure with an inner hexagonal concentric cylinder in the Rayleigh number range of 10^2 to 10^5. In their work, the velocity component in computational coordinate and that in physical coordinate were adopted as the primary independent variables. Elepano and Oosthuizen [3], studied natural convective flow in an enclosure containing a heated cylinder and a cooled upper surface numerically. They used stream function–vorticity formulation and the finite element technique to solve the governing equations. Oosthuizen and Paul [4], studied numerically, two-dimensional free convective flow in an enclosure which has a heated half-cylinder, kept at uniform high temperature. The enclosure has a horizontal upper and lower walls and inclined side walls. The side walls are kept at uniform temperatures and the top surface was considered adiabatic. They concluded that, when the flow in the enclosure was symmetrical about the vertical center-line of the enclosure, the dimensionless height of the enclosure was the only geometric parameter that had a significant effect on the mean heat transfer rate from the half-cylinder at a given Rayleigh number. Fu et al. [5] studied numerically natural convection of an enclosure by a rotating circular cylinder near a hot wall using a finite element method. They showed that the rotating cylinder direction had an important effect in enhancing natural convection heat transfer in the enclosure. Fu and Tong [6], numerically studied the flow structures and heat transfer characteristics of a heated cylinder oscillating transversely. They showed that

☆ Communicated by W.J. Minkowycz.

* Corresponding author.
E-mail addresses: salamphd1974@yahoo.com (S.H. Hussain), ahmedkadhim74@yahoo.com (A.K. Hussein).

0735-1933/$ – see front matter © 2010 Elsevier Ltd. All rights reserved.
doi:10.1016/j.icheatmasstransfer.2010.12.006

Nomenclature

D	Rotating circular cylinder diameter, (m)
g	Gravitational acceleration, (m/s^2)
k	Thermal conductivity of fluid, (W/m °C)
k_s	Thermal conductivity of rotating cylinder, (W/m.°C)
K	Solid–fluid thermal conductivity ratio
L	Width or height of the enclosure, (m)
Nu_{av}	Average Nusselt number
P	Dimensionless pressure
p	Pressure, (N/m^2)
Pr	Prandtl number
R	Radius of rotating circular cylinder, (m)
Ra	Rayleigh number
Re	Reynolds number
T	Temperature, (°C)
T_c	Temperature of the cold surface, (°C)
T_h	Temperature of the hot surface, (°C)
T_s	Temperature of cylinder surface, (°C)
U	Dimensionless velocity component in x-direction
u	Velocity component in x-direction, (m/s)
V	Dimensionless velocity component in y-direction
v	Velocity component in y-direction, (m/s)
X	Dimensionless coordinate in horizontal direction
x	Cartesian coordinate in horizontal direction, (m)
Y	Dimensionless coordinate in vertical direction
y	Cartesian coordinate in vertical direction, (m)

Greek symbols

α	Thermal diffusivity, (m^2/s)
β	Volumetric coefficient of thermal expansion, (K^{-1})
θ	Dimensionless temperature
θ_s	Dimensionless temperature of rotating cylinder
ϑ	Kinematic viscosity of the fluid, (m^2/s)
ρ	Density of the fluid, (kg/m^3)
δ	distance from center of square cylinder to circular cylinder center, (m)
ω	Angular rotational velocity, (rad/s)

the interaction between the oscillating cylinder and the vortex shedding dominated the state of the wake and the flow and the thermal fields may approached a periodic state in the lock-on regime at which the heat transfer was enhanced remarkably. Ha et al. [7] and [8] considered the problem of natural convection in a square enclosure with isothermal top and bottom boundaries and adiabatic side walls. A square cylinder was placed at the center of the enclosure and different boundary conditions were considered for this internal cylinder. A wide range of Rayleigh numbers was considered extending from the steady regime to that of highly chaotic turbulence. The effect of the internal square body and its thermal boundary condition on the nature of convection and overall heat transfer was investigated. Roychowdhury et al. [9], used a collected, non-orthogonal grid based on finite volume technique to investigate the two-dimensional natural convective flow and heat transfer around a heated cylinder kept in a square enclosure. The effects of different enclosure wall thermal boundary conditions, fluid Prandtl number and the ratio between enclosure and cylinder dimensions were also studied. It was observed that the patterns of recirculatory flow and thermal stratification in the fluid are significantly modified, if any of the considered parameters are varied. De and Dalal [10], studied numerically natural convection around a tilted heated square cylinder kept in an enclosure in the range of $10^3 \le Ra \le 10^6$. Stream function–vorticity formulation of the Navier–Stokes equations was solved numerically using finite-difference method. It was found that the uniform wall temperature heating was quantitatively different from the uniform wall heat flux heating. Flow pattern and thermal stratification were modified, if aspect ratio was varied. Also, it was found that the overall heat transfer also changed for different aspect ratios. Angeli et al. [11], investigated numerically buoyancy-induced flow regimes of a horizontal cylinder centered into a long co-axial square-sectioned cavity. Substantial differences were observed in the flow and thermal fields, depending on the aspect ratio and the Rayleigh number, in the regions of either asymptotically steady or time-dependent flows. A correlating equation for the average Nusselt number on the cylinder, as a function on both the Rayleigh number and the diameter-to-side ratio was derived which covering the whole steady-state region. Hwang et al. [12], studied the flow field around an infinitely long circular cylinder rotating in fluid with no outer boundary. The governing equations were discretized by using a finite-volume method on a cylindrical grid system. Wall pressure fluctuations are found to be of much larger spatial extent than velocity fluctuation scales. Rahman et al. [13], performed a numerical investigation of laminar mixed convection in a square cavity with a heat conducting horizontal square cylinder to investigate the effect of the locations of the conducting cylinder on the fluid flow and heat transfer in the square cavity for different Richardson numbers in the range of $0 \le Ri \le 5$ .The results indicated that, the cylinder locations had a significant effect on the flow and thermal fields and the value of average Nusselt number was the highest in the forced convection dominated area when the cylinder was located near the top wall along the mid-vertical plane and in the free convection dominated area when the cylinder moved closure to the left vertical wall along the mid-horizontal plane. Ghazanfarian and Nobari [14] presented a numerical investigation of convective heat transfer from a rotating cylinder with cross-flow oscillation. A finite element analysis using *C*haracteristic *B*ased *S*plit method (CBS) was developed to solve governing equations. It was found that similar to the fixed cylinder, beyond a critical rotating speed, vortex shedding was mainly suppressed. Also by increasing the non-dimensional rotational speed of the cylinder, both the Nusselt number and the drag coefficient decreased rapidly. Shih et al. [15], investigated numerically the periodic state of fluid flow and heat transfer due to isothermal or adiabatic rotating cylinder enclosed in a square cavity. By comparing the time-averaged Nusselt numbers of the system for both adiabatic and isothermal objects, it was concluded that for high Reynolds number cases, heat transfer was independent of the shape of the object. Yoon et al. [16], presented a numerical investigation of the characteristics of the two-dimensional laminar flow around two rotating circular cylinders in side-by-side arrangements. Numerical simulations are performed for various ranges of absolute rotational speeds at Reynolds number of 100. Quantitative information about the flow variables such as the pressure coefficient and wall vorticity distributions on the cylinders was highlighted. Paramane and Sharma [17], analysed convection heat transfer across a circular cylinder rotating with a constant non-dimensional rotation rate varying from 0 to 6 for Reynolds numbers of 20–160 and a Prandtl number of 0.7.They concluded that, the average Nusselt number decreased with increasing rotation rate and increased with increasing Reynolds number. It was also found that, the heat transfer suppression due to rotation increased with increasing Reynolds number and rotation rate. Oztop et al. [18], studied mixed convection heat transfer characteristics for a lid-driven air flow within a square enclosure having a circular body. The cavity was differentially heated and the left wall was maintained at a higher temperature than the right wall. Three different temperature boundary conditions were applied for the inner cylinder as adiabatic, isothermal or conductive. The computation was carried out for wide ranges of Richardson numbers, diameter of inner cylinder and center and location of the inner cylinder. It was found that, the thermal conductivity became insignificant for small values of diameter of the circular body and the circular body can be used as a control parameter for heat and fluid flow. Rahman et al. [19], studied numerically combined free and forced convection in a two dimensional

rectangular cavity with a uniform heat source applied on the right vertical wall. A circular heat conducting horizontal cylinder was placed somewhere within the cavity. The results indicated that both the heat transfer rate from the heated wall and the dimensionless temperature in the cavity strongly depended on the governing parameters and configurations of the system studied, such as size, location, thermal conductivity of the cylinder and the location of the inflow and outflow opening. Yoon et al. [20], carried out a numerical calculations for the natural convection induced by temperature difference between a cold outer square enclosure and a hot inner circular cylinder for Rayleigh number of $Ra=10^7$. Their study investigated the effect of the inner cylinder location on the heat transfer and fluid flow. They concluded that, at the unsteady region, the natural convection showed a single frequency and multiple frequency periodic patterns alternately according to the location of inner circular cylinder. Costa and Raimundo [21], studied mixed convection in a differentially heated square enclosure with a rotating cylinder inside it. The flow structure, the temperature field and the heat transfer process were analyzed using the dimensionless stream function, temperature and heat function. It was observed that the size of the cylinder had a strong influence on the resulting flow and heat transfer process, as it limited the space for fluid flow between the cylinder and the enclosure walls. They concluded that, for high values of the cylinder radius, the overall Nusselt number was small if the rotating velocity was low. Mohammed and Salman [22] studied experimentally laminar combined natural and forced convection heat transfer in a uniformly heated vertical circular cylinder for assisting flow with different entrance sections length under constant wall heat input. The results clearly showed that the surface temperature values decreased as the cylinder inclination angle moved from $\theta=90°$ (vertical cylinder) to $\theta=0°$ (horizontal cylinder). Laskowski et al. [23] studied both experimentally and numerically heat transfer to and from a circular cylinder in a cross-flow of water at low Reynolds number. The cylinder was placed near the lower surface of a water channel. The results explained that the predicted spatially averaged Nusselt number was from 37% to 53% larger than the measured spatially averaged Nusselt number. Champigny et al. [24] characterized the mixed convection flows and its associated heat transfers, in the frame of the nuclear waste management. The main issue was the design of the storage facilities with great confidence, using tools validated with the experiment results. The air flow profiles and the cylinder wall temperatures issued from numerical calculations are analyzed and the results are compared with the experimental ones. Recently, Hussain and Hussein [25] investigated numerically the laminar steady natural convection where a uniform heat source applied on the inner circular cylinder enclosed in a square enclosure in which all boundaries are assumed to be isothermal .They concluded that with increasing Rayleigh number, the average and local Nusselt number values increased with different upward and downward locations of the inner cylinder, due to the significant influence of thermal convection. Very recently, Saha et al. [26] studied numerically the problem of two-dimensional laminar mixed convection in a tilted lid-driven square enclosure in the presence of adiabatic cylinder at the center using the combined finite element method. The results indicated that the flow and thermal fields eventually reached the steady state with the symmetric shape about the vertical centerline through the center of the inner circular cylinder. However, so far there is no study related with heat transfer characteristics of the flow and thermal fields past a rotating conductive circular cylinder with combined convection heat transfer flow of air in a differentially heated square enclosure at different vertical locations. This is the main concern of the present paper. Here, a numerical scheme is constructed using a finite volume approach to deal with a laminar steady combined convection problem in a two-dimensional square enclosure which contains a rotating conductive circular cylinder of radius ($R=0.2$ L) enclosed inside it. The numerical calculations are performed for wide ranges of Reynolds and Richardson numbers, the solid–fluid thermal conductivity ratios and inner rotating circular cylinder location (δ).

2. Configuration description and mathematical model

The present configuration consists of a two-dimensional square enclosure of the same height and width (L). A circular solid conductive rotating cylinder with radius ($R=0.2$ L) and thermal conductivity, (k_s) is placed in the center of square enclosure and rotates with an angular velocity (ω) in counterclockwise direction. The physical model considered here is shown in Fig. 1 along with the important geometric parameters. A Cartesian coordinate is used with origin at the lower left corner of the computational domain. Air is considered as the fluid inside the square enclosure with $Pr=0.71$.The cylinder moves along the vertical centerline of the enclosure in the range from -0.25 L to $+0.25$ L. The upper and lower horizontal walls of the enclosure are considered to be adiabatic, while the vertical side left wall is subjected to an isothermal temperature higher than the opposite right side wall. All solid boundaries are assumed to be no-slip rigid walls. The Reynolds and Richardson numbers are considered in the ranges 50 to 300 and from 0 to 10 respectively, while the solid–fluid thermal conductivity ratios are taken as 0.2, 1, 5 and 10. All fluid properties are assumed constant except for the density variation in the buoyancy term which is treated according to Boussinesq approximation. The radiation effects are neglected and the gravitational acceleration acts in the negative y-direction. The fluid within the enclosure is assumed incompressible and Newtonian while viscous dissipation effects are considered negligible. The flow and thermal fields inside the square enclosure with a rotating circular cylinder are described by the Navier–Stokes and the energy equations, respectively. The governing equations are transformed into a dimensionless form under the following non-dimensional variables [13]:

$$\theta=\frac{T-T_c}{T_h-T_c},\ \theta_s=\frac{T_s-T_c}{T_h-T_c},\ X=\frac{x}{L},\ Y=\frac{y}{L}$$
$$U=\frac{u}{\omega R},\ V=\frac{v}{\omega R},\ P=\frac{p}{\rho(\omega R)^2},\ Pr=\frac{\nu}{\alpha},$$
$$Re=\frac{\rho(\omega R)D}{\mu},\ Gr=\frac{g\beta(T_h-T_c)L^3}{\vartheta^2}\ \text{and}\quad (1)$$
$$Ri=\frac{Gr}{Re^2}$$

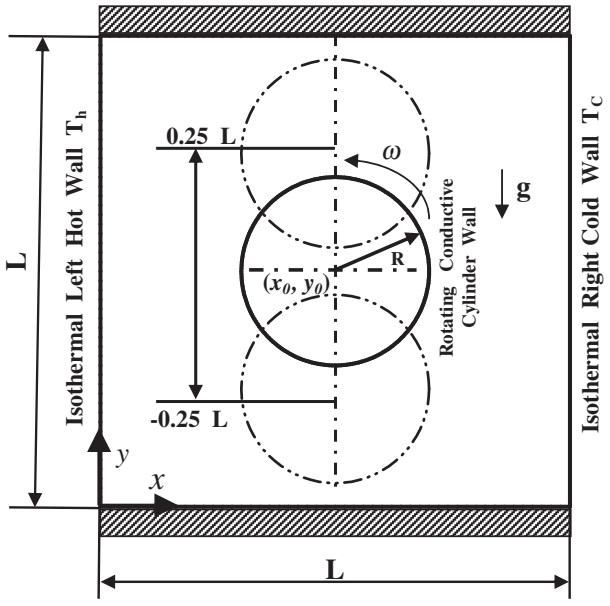

Fig. 1. Schematic diagram of the square enclosure with inner rotating conductive circular cylinder with counterclockwise direction along with coordinate system and boundary conditions.

where X and Y are the dimensionless coordinates measured along the horizontal and vertical axes, respectively, u and v being the dimensional velocity components along x and y axes, and θ is the dimensionless temperature. β is the volumetric coefficient of thermal expansion and g is the gravitational acceleration. The dimensionless forms of the governing equations under steady state condition are expressed in the following forms [13]:

$$\frac{\partial U}{\partial X} + \frac{\partial V}{\partial Y} = 0 \tag{2}$$

$$U\frac{\partial U}{\partial X} + V\frac{\partial U}{\partial Y} = -\frac{\partial P}{\partial X} + \frac{1}{Re}\left(\frac{\partial^2 U}{\partial X^2} + \frac{\partial^2 U}{\partial Y^2}\right) \tag{3}$$

$$U\frac{\partial V}{\partial X} + V\frac{\partial V}{\partial Y} = -\frac{\partial P}{\partial Y} + \frac{1}{Re}\left(\frac{\partial^2 V}{\partial X^2} + \frac{\partial^2 V}{\partial Y^2}\right) + Ri\,\theta \tag{4}$$

$$U\frac{\partial \theta}{\partial X} + V\frac{\partial \theta}{\partial Y} = \frac{1}{Re\,Pr}\left(\frac{\partial^2 \theta}{\partial X^2} + \frac{\partial^2 \theta}{\partial Y^2}\right) \tag{5}$$

For heat conducting cylinder, the energy equation is

$$\left(\frac{\partial^2 \theta_s}{\partial X^2} + \frac{\partial^2 \theta_s}{\partial Y^2}\right) = 0 \tag{6}$$

Non-dimensional forms of the boundary conditions for the present problem are specified as follows:

At all solid boundaries of the square enclosure: $U=0$, $V=0$

At the heated left vertical wall: $\theta=1$

At the cooled right vertical wall: $\theta=0$

At the upper and lower walls:

$$\frac{\partial \theta}{\partial Y}\Big|_{Y=1,0} = 0$$

At the solid–fluid vertical interfaces of the block: $\left(\frac{\partial \theta}{\partial X}\right)_{fluid} = K\left(\frac{\partial \theta}{\partial X}\right)_{solid}$

At the solid–fluid horizontal interfaces of the block: $\left(\frac{\partial \theta}{\partial Y}\right)_{fluid} = K\left(\frac{\partial \theta}{\partial Y}\right)_{solid}$

Over the rotating cylinder, velocity components are specified as [21]:

$$u = \omega(y - y_0) \tag{7a}$$

$$v = \omega(x - x_0) \tag{7b}$$

At any point of the cylinder, the absolute value of the velocity can be evaluated as [21]:

$$|V| = \sqrt{u^2 + v^2} \tag{8a}$$

$$|V| = \sqrt{\omega^2(y-y_0)^2 + \omega^2(x-x_0)^2} \tag{8b}$$

$$|V| = |\omega| r \tag{8c}$$

In particular, over the surface of the cylinder it is $|V| = |\omega| R$ and Eqs. (7a) and (7b) apply with the coordinates x and y corresponding to the surface points. The average Nusselt number (Nu) at the hot wall is defined as [13] :

$$Nu_{av} = \int_0^1 \frac{\partial \theta}{\partial X}\Big|_{X=0} dY \tag{9}$$

3. Computational procedure

A numerical solution procedure is adopted, which is based upon finite volume method to discretize the system of steady elliptic equations on a collocated grid system, and the details can be found in the text by Ferziger and Peric [27]. A typical grid distribution (200×100) with non-uniform and non-orthogonal distributions for $\delta=0$ is shown in Fig. 2. The third-order deferred correction QUICK scheme and second-order central difference scheme are, respectively, implemented for the convection and diffusion terms. The resulting discretized equations are solved using the strongly implicit procedure (SIP) of Stone [28]. The pressure–velocity link is established through the SIMPLE algorithm [29]. The fluid and solid regions are solved simultaneously by introducing a block parameter, which distinguishes the solid region from the fluid region, into discretized governing Eqs. ((3) and (4)), which would make the velocity negligibly small in solid region by solving momentum equations. Thus the continuity equation (Eq. (2)) is automatically satisfied. Accordingly, the energy equation (Eq. (5)) is reduced to heat conduction equation (Eq. (6)) for the solid region, because the convection terms in energy equation (Eq. (5)) are automatically turned off. By combining the energy equations in this manner, the matching conditions at the fluid/solid interface are satisfied automatically. The algorithm ensures continuity of the fluxes across all the control surfaces, and thus, the fluid–solid interfaces. The coupled convection and conduction analysis lie in that the same set of conservative equations [Eqs. (2)–(6)] which is simultaneously solved over the entire domain including both fluid and solid regions. The convergence criterion is the maximal residual of all the governing equations which is less than 10^{-7}. In addition to the usual accuracy control, the accuracy of computations is also controlled using the energy conservation within the system.

4. Grid refinement check

In order to obtain grid independent solution, a grid refinement study is performed for a square enclosure with the horizontal conductive circular cylinder at $Re=300$, $Ri=10$, $K=10$ and $\delta=+0.25$. In the present work, eight combinations (70×70, 80×80, 100×80, 100×100, 120×120, 200×100, 200×200 and 300×300) of non-uniform grids are used to test the effect of grid size on the accuracy of the predicted results. Fig. 3 shows the convergence of the average Nusselt number (Nu_{av}), at the heated left wall with grid refinement. It is observed that grid independence is achieved with

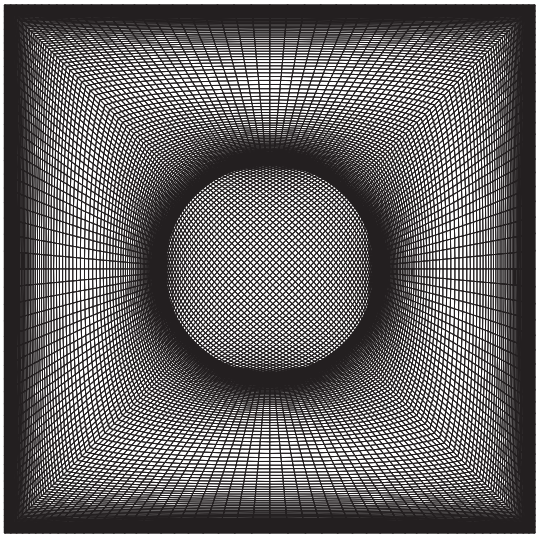

Fig. 2. A typical grid distribution (200×100) with non-uniform and non-orthogonal distributions for $\delta=0$.

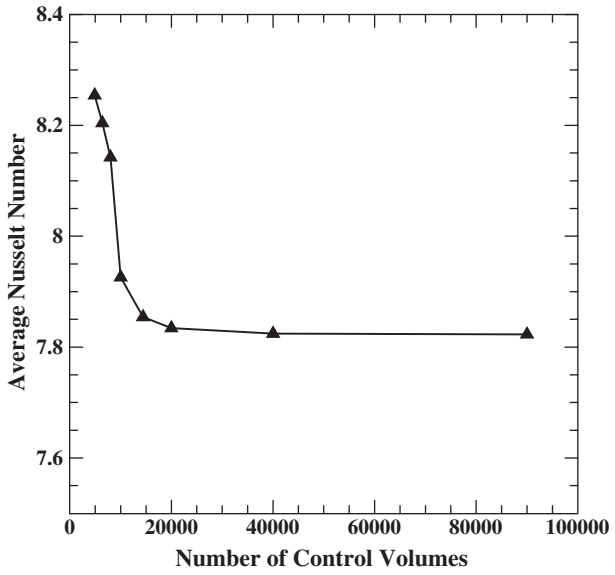

Fig. 3. Convergence of average Nusselt number along the heated left wall of the square enclosure with grid refinement for $Re=300$, $Ri=10$, $Pr=0.7$, $K=10$ and $\delta=+0.25$.

combination of (120×120) control volumes where there is insignificant change in the average Nusselt number (Nu_{av}) with the improvement of finer grid. The agreement is found to be excellent which validates the present computations indirectly. Hence, for the rest of the calculation in this study, a grid size of (120×120) control volumes is chosen for optimum results.

5. Numerical results verification

To check the adequacy of the numerical scheme, the natural convection problem for a low temperature outer square enclosure and high temperature inner circular cylinder was tested. The calculated surface-averaged Nusselt numbers for the test case are compared with the benchmark values by Kim et al. [30] and Moukalled and Acharya [31] as shown in Table 1. Further verification was performed by using the present numerical algorithm to investigate the same problem considered by Kim et al. [30] using the same flow conditions and geometries, which were reported for laminar natural convection heat transfer using the same boundary conditions but the numerical scheme is different. The comparison is made using the following dimensionless parameters: $Pr=0.7$, $Ra=10^3-10^6$ and $\delta=0$. Excellent agreement was achieved between Kim et al. [30] results and the present numerical scheme results for both the streamlines and temperature contours inside the square enclosure with the inner cylinder along the horizontal centerline at $\delta=0$ as shown in Fig. 4. These verifications make a good confidence in the present numerical model to deal with the other vertical centerline locations (δ's).

Table 1
Comparison of present surface-averaged Nusselt number with those of previous studies.

Ra	Mean Nusselt number at the hot wall			Error (%)
	Present study	Kim et al. [30]	Moukalled and Acharya [31]	
10^4	3.40470	3.4140	3.331	−2.21250
10^5	5.12893	5.1385	5.080	−0.96318
10^6	9.38875	9.3900	9.374	−0.15730
10^7	15.6995	15.665	15.790	0.57314

6. Results and discussion

The basic features of the flow and thermal fields in a square enclosure of same height and width, with a conductive rotating solid circular cylinder of radius ($R=0.2$ L) enclosed inside it, is investigated in this section with the help of isotherms and the streamline patterns. In the current numerical work, the following ranges of the dimensionless groups are considered: The working fluid is air with Prandtl number (Pr) = 0.71, the ranges of the Richardson numbers are 0,1, 5 and 10, while Reynolds numbers are taken as 50, 100, 200 and 300 respectively. The solid–fluid thermal conductivity ratios (K) are taken as 0.2, 1, 5 and 10. Figs. 5 and 6, show the streamlines and isotherms variation for different values of Richardson number and inner rotating circular cylinder location (δ) when the solid–fluid thermal conductivity ratio (K) is 5 and Reynolds number $Re=50$ and $Re=300$ respectively as a representative case. The figures explain that, when the air inside the square enclosure touches the conductive rotating circular cylinder, it becomes hotter and lighter due to high thermal conductivity effect of the inner cylinder. The air is lifted and try to move around the conductive rotating circular cylinder until it contacts the adiabatic top wall of the enclosure. The hot air near the adiabatic top wall becomes colder and then moves adjacent to the right cold side wall which changing its direction of flow leading to produce a rotating identical vortices around the conductive rotating circular cylinder. When the Richardson number is small (i.e., $Ri=0$), which represents the forced convection case. The buoyancy force effect is small, so for this case the natural convection contribution is small also. Major rotating vortices can be noticed around the solid rotating circular cylinder which is almost identical at $\delta=0$, where the rotating cylinder locates at the center of the square enclosure. The inner rotating circular cylinder locations (δ) has a small effect on the flow patterns and isotherms when the rotating circular cylinder moves upward until $\delta=+0.1$, or when it moves downward until $\delta=-0.1$, where the flow patterns and isotherms are almost identical in this case. A very small minor vortices can be detected near the corners of the square enclosure, due to the domination of forced convection. This behaviour refers that the heat transfer process is insensitive to rotating circular cylinder locations (δ) in the range $-0.1\le\delta\le+0.1$, when the Richardson number is small. When the inner rotating circular cylinder locations (δ) increases up to $\delta=+0.25$ (i.e., when the rotating circular cylinder moves upward) or decreases until it reaches $\delta=-0.25$ (i.e., when the rotating circular cylinder moves downward) a different behaviour can be noticed in the streamlines and isotherm contours where a major rotating vortices appear down the rotating cylinder when the cylinder moves upward or up the rotating cylinder when it moves downward. Also, the major vortices are increase in size, while the small minor vortices began to disappear when the cylinder moves in the ranges $-0.15\le\delta\le-0.25$ and $+0.15\le\delta\le+0.25$ .Moreover, the temperature contours become more confused at this ranges. In general, it can be observed, that the temperature contours approximately parallel and symmetrical adjacent to the left hot side wall of the enclosure indicating that the conduction heat transfer has become the dominant mode of energy transport in the square enclosure. When the Richardson number is unity (i.e., $Ri=1$), the heat transfer mechanism in the square enclosure is occurred by the combined mechanisms of natural and forced convection (i.e., the mixed convection is dominant).In this situation, the buoyancy forces effect balances the effect of the rotating circular cylinder. No clear changes can be noticed in the streamlines and isotherm contours with the rotating circular cylinder locations (δ) since they are similar with the corresponding streamlines and isotherm contours at the previous case when the Richardson number is $Ri=0$.When the Richardson numbers are 5 and 10 respectively, the buoyancy forces effect becomes greater than the effect of the rotating circular cylinder, so the natural convection is dominant. At this case, a dramatic changes occur in the rotating vortices which become

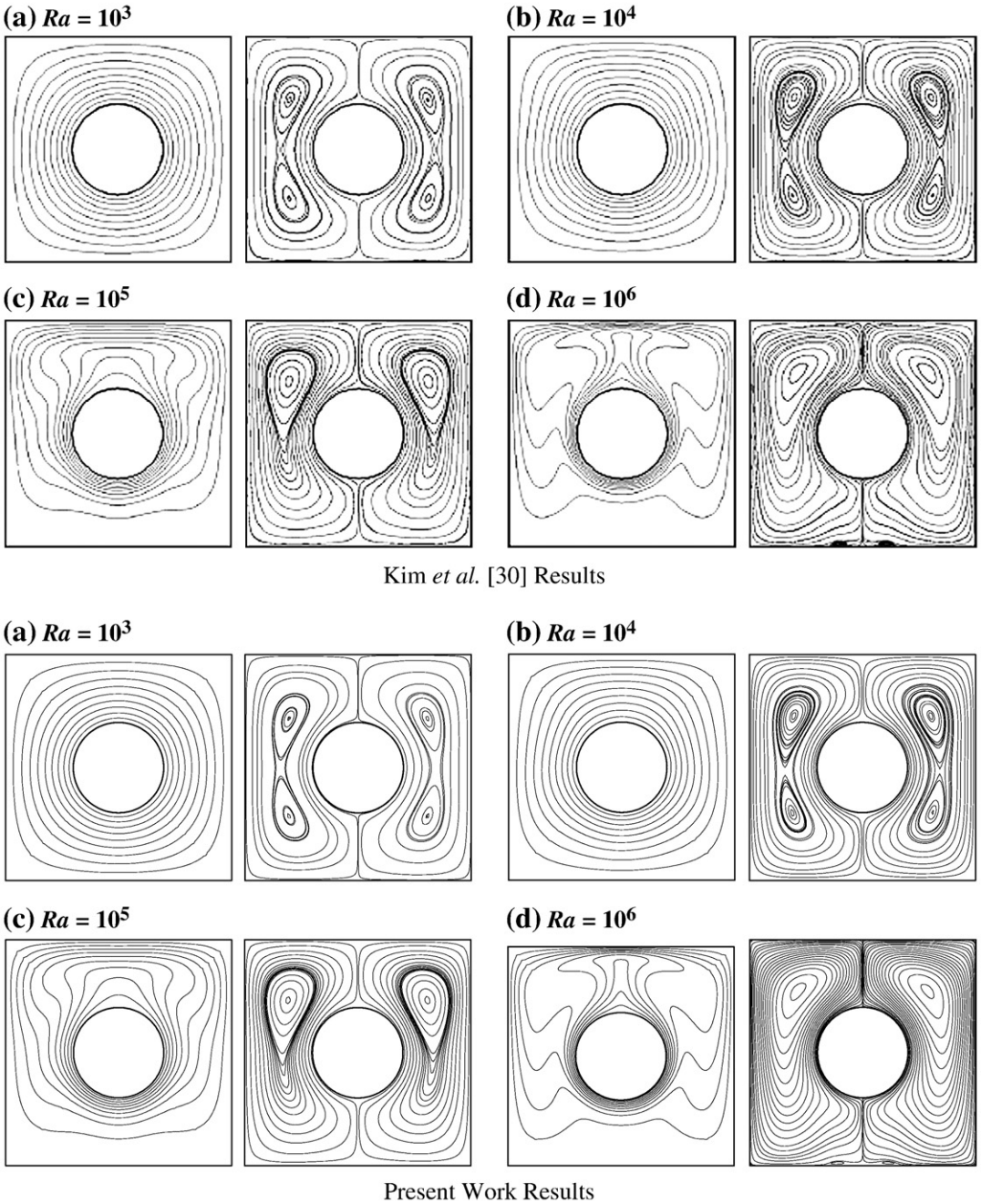

Fig. 4. Comparison of the temperature contours and streamlines between the present work and that of Kim et al. [30], at $\delta = 0$ for four different Rayleigh numbers of (a) 10^3, (b) 10^4, (c) 10^5 and (d) 10^6.

irregular, slightly large in pattern and size as the solid rotating circular cylinder moves downward in the direction of the bottom wall (i.e., the values of δ decrease), or when the solid rotating circular cylinder moves upward in the direction of the upper wall (i.e., the values of δ increase) and as a result making a large convection heat transfer contribution. It is observed that the small minor vortices at the upper and lower edges of the square enclosure are increased in size, when the solid rotating circular cylinder moves upward in the domain $0 \leq \delta \leq +0.1$ or, when it moves downward in the domain $-0.1 \leq \delta \leq 0$. This is because the buoyancy force dominates the forced convective flow in the square enclosure. After that, these minor vortices begin to decrease in size gradually. Also, when the Richardson numbers are 5.0 and 10 respectively, the isothermal lines become non-symmetry, non-uniformly distributed and more concentrated adjacent to the left hot side wall of the square enclosure, since the buoyancy forces effect on the flow and thermal fields becomes more significant with increasing of Richardson number and as a result the heat is transferred due to convection. Moreover, it can be observed that some isotherm lines pass through the rotating circular cylinder for most of considered cases, which refers that a part of heat comes from the hot left side wall of the square enclosure passing through the rotating circular cylinder and then go back secondly to the fluid enclosed in the enclosure. When, the Reynolds number increases from 50 in Fig. 5 to 300 as shown in Fig. 6, the role of the angular rotational velocity of the rotating solid circular cylinder becomes clear dominant, since the Reynolds number is directly proportional to the angular rotational velocity (ω). Due to this reason, the circulation of flow vortices increases dramatically and becomes more stronger ,which leads to make the forced convection effect more dominant. It can be observed that, intensity of the vortices circulation becomes more concentrated

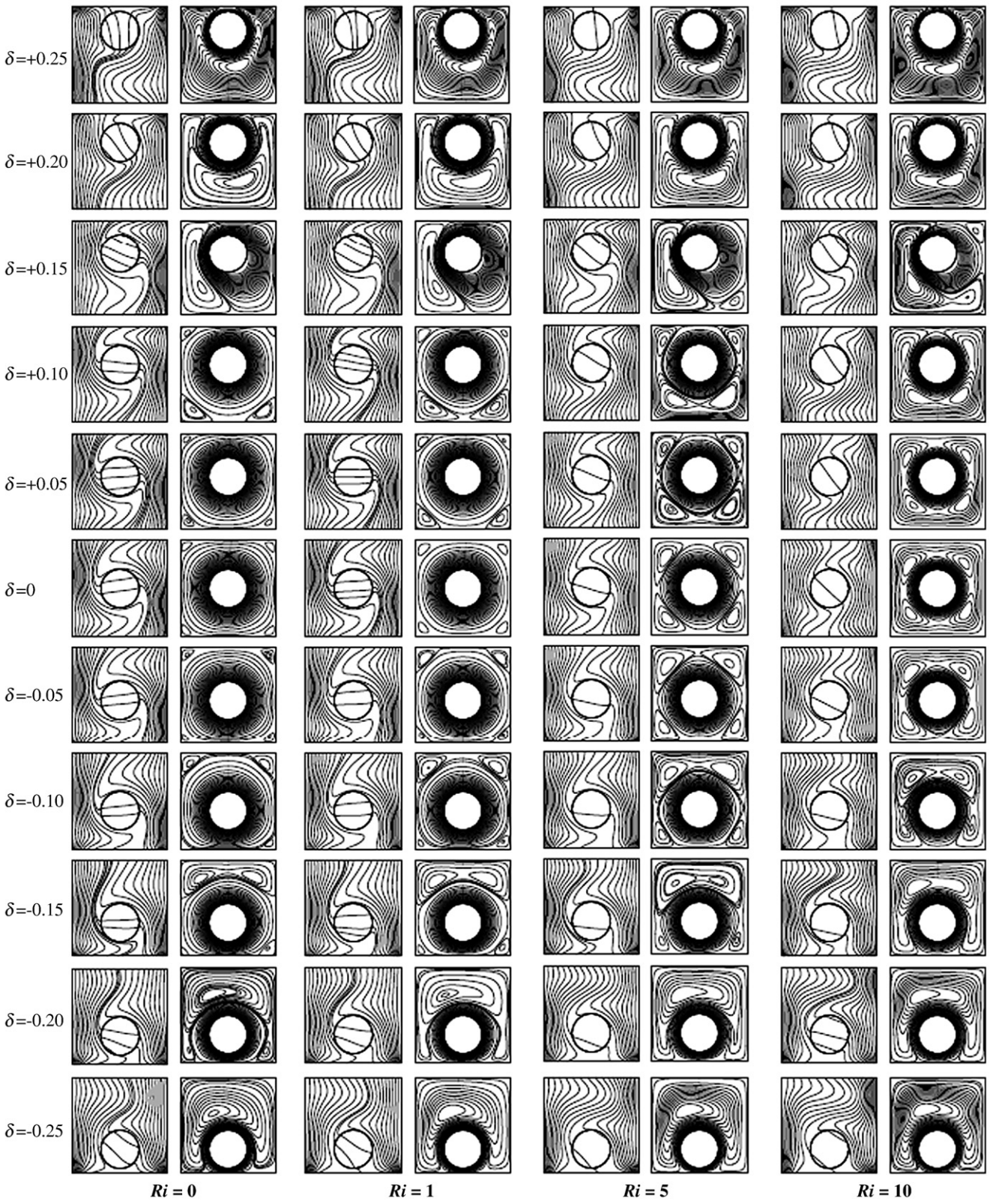

Fig. 5. Isotherm (left) and streamlines (right) for different values of *Ri* and δ while $K=5$ and $Re=50$.

and covers most of the enclosure size for different values of Richardson numbers and rotating circular cylinder locations (δ) comparing with the corresponding vortices when the Reynolds number is 50 as shown in Fig. 5.The reason of this behaviour, is due to small role of angular rotational velocity of the rotating solid circular cylinder, when the Reynolds number is small. From the other hand, the isotherm lines become more thicker and occupy almost the whole enclosure, when the Reynolds number is 300.This leads to increase the heat transfer effect by the rotating solid circular cylinder ,and as a result more heat can be transferred from the rotating solid circular cylinder and dissipated uniformly inside the square enclosure. Also, a thin thermal boundary layer is created and can be observed easily

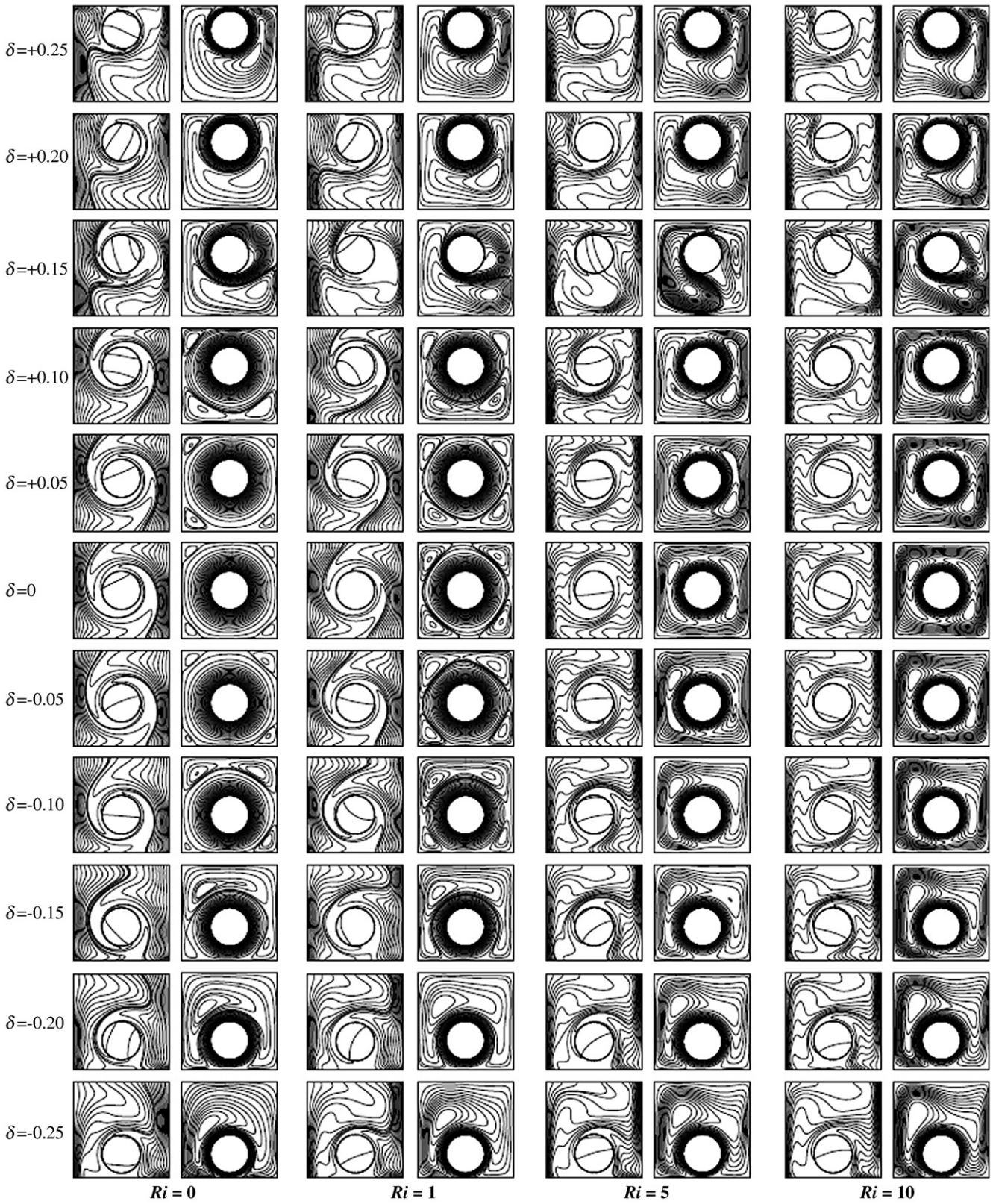

Fig. 6. Isotherm (left) and streamlines (right) for different values of *Ri* and δ while $K=5$ and $Re=300$.

near the left hot side wall, when the Reynolds number is 300 as shown in Fig. 6. The effect of the solid–fluid thermal conductivity ratios (K) on the flow and thermal fields for different Richardson numbers, $Re=200$ and three values of inner rotating circular cylinder location (δ) which are -0.25, 0 and $+0.25$ as a representative case is explained in Fig. 7. For the selected range of solid–fluid thermal conductivity ratios (K) which are taken as 0.2, 1, 5 and 10 respectively, it can be observed that for each value of (δ), no clear change can be observed in the streamlines, which indicates that the solid–fluid thermal conductivity ratios (K) have a slight effect on the flow field.

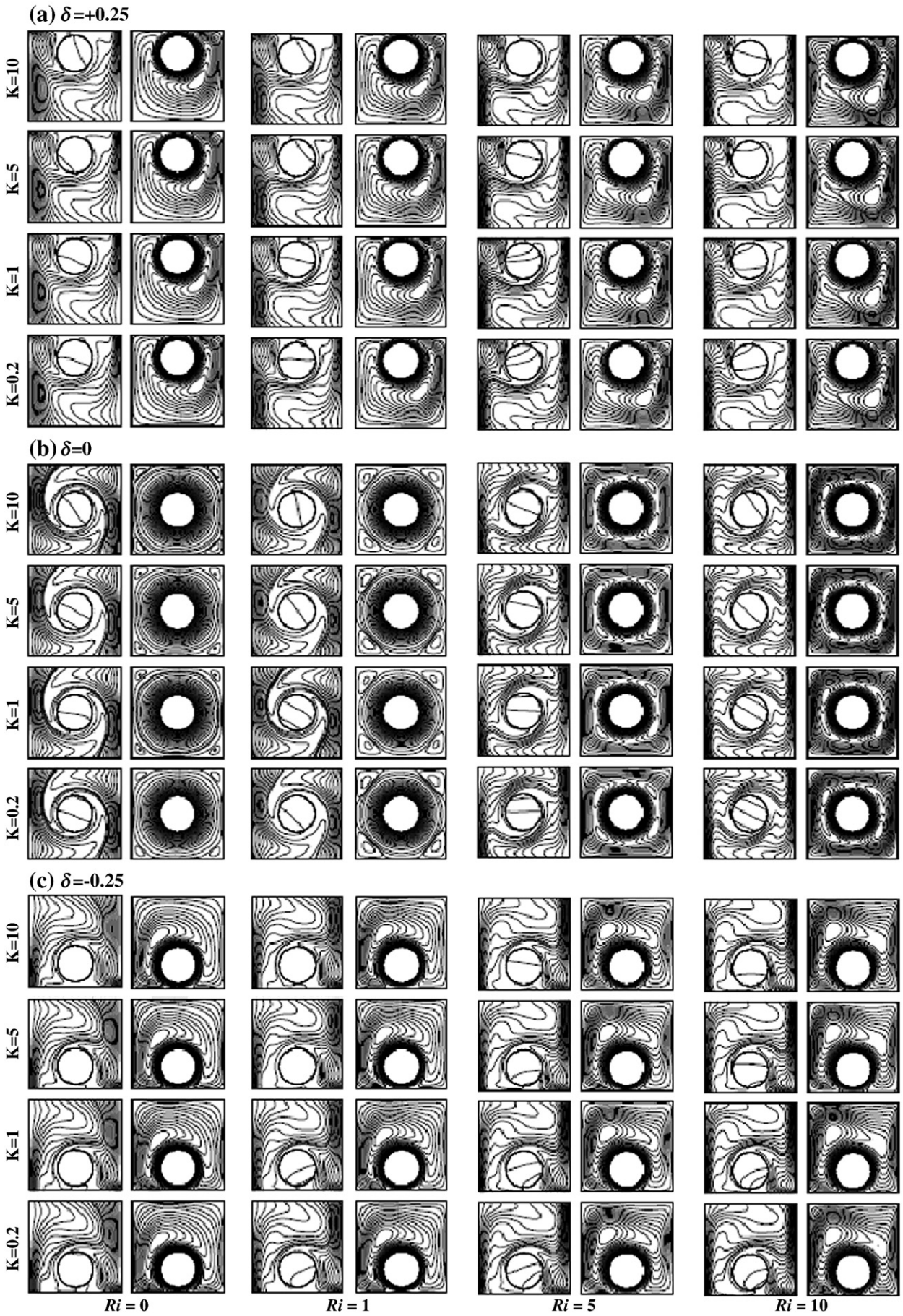

Fig. 7. Isotherm (left) and streamlines (right) for different values of *K*, *Ri* and δ while $Re = 200$.

From the other hand, the main influence of solid–fluid thermal conductivity ratios (K) occurs on the isotherm lines, which are related with the growth of thermal boundary layer. This can be observed clearly adjacent to the left hot side wall of the square enclosure. The thermal boundary layer can be noticed for all selected values of (δ) and Richardson numbers. It becomes more thicker with increasing of Richardson number. Fig. 8, shows the average Nusselt number plots at the hot left side wall against the inner rotating circular cylinder location (δ) for different Richardson and Reynolds numbers. The figure shows that the average Nusselt number value increases as the Reynolds number increases. The reason of this behaviour, since the isotherm lines become more thicker and concentrate with the Reynolds numbers increasing which leads to increase the rotating circular cylinder heat transfer contribution and as a result more heat transfer occurs from the rotating circular cylinder and dissipates uniformly inside the square enclosure causing an increase in the average Nusselt number values. From the other hand, the average Nusselt numbers increase as the Richardson number increases for selected values of (δ). The reason of this behaviour, since for high values of Richardson number, the isotherm lines goes to change and become non- uniformly and highly concentrated at the hot left side wall of the enclosure due to high temperature gradient at this region. Therefore, the heat is strongly transferred by natural convection currents and this leads normally to increase the average Nusselt number values. Also, when the values of (δ) decrease (i.e., when the rotating cylinder moves downward) or when the values of (δ) increase (i.e., when the rotating cylinder moves upward), the average Nusselt number adjacent to the hot left side wall begins with a high value due to strong convection vortices and then gradually decreases. After that, the average Nusselt number increases secondly until it reaches a high value in the range ($-0.1 \le \delta \le +0.1$) due to great effect of convection. Moreover, the average Nusselt number, increases rapidly and highly in the range ($0.2 \le \delta$). This due to concentration of isotherm lines in a very small zone leading to increase the average Nusselt number values. The average Nusselt numbers at the hot left side wall have been plotted as a function of Richardson number for different values of solid–fluid thermal conductivity ratios (K) and some selected values of (δ) at $Re = 200$ as shown in Fig. 9. From this figure, it can be observed that no significant effect of solid–fluid thermal conductivity ratios (K) on the average Nusselt number values. Again, the average Nusselt number increases as the Richardson number increases with selected upward and downward rotating circular cylinder locations, due to the great influence of thermal convection heat transfer. Also, it can be observed that, at the hot left side wall of the enclosure when the solid–fluid thermal conductivity ratio decreases the average Nusselt number increases. The main

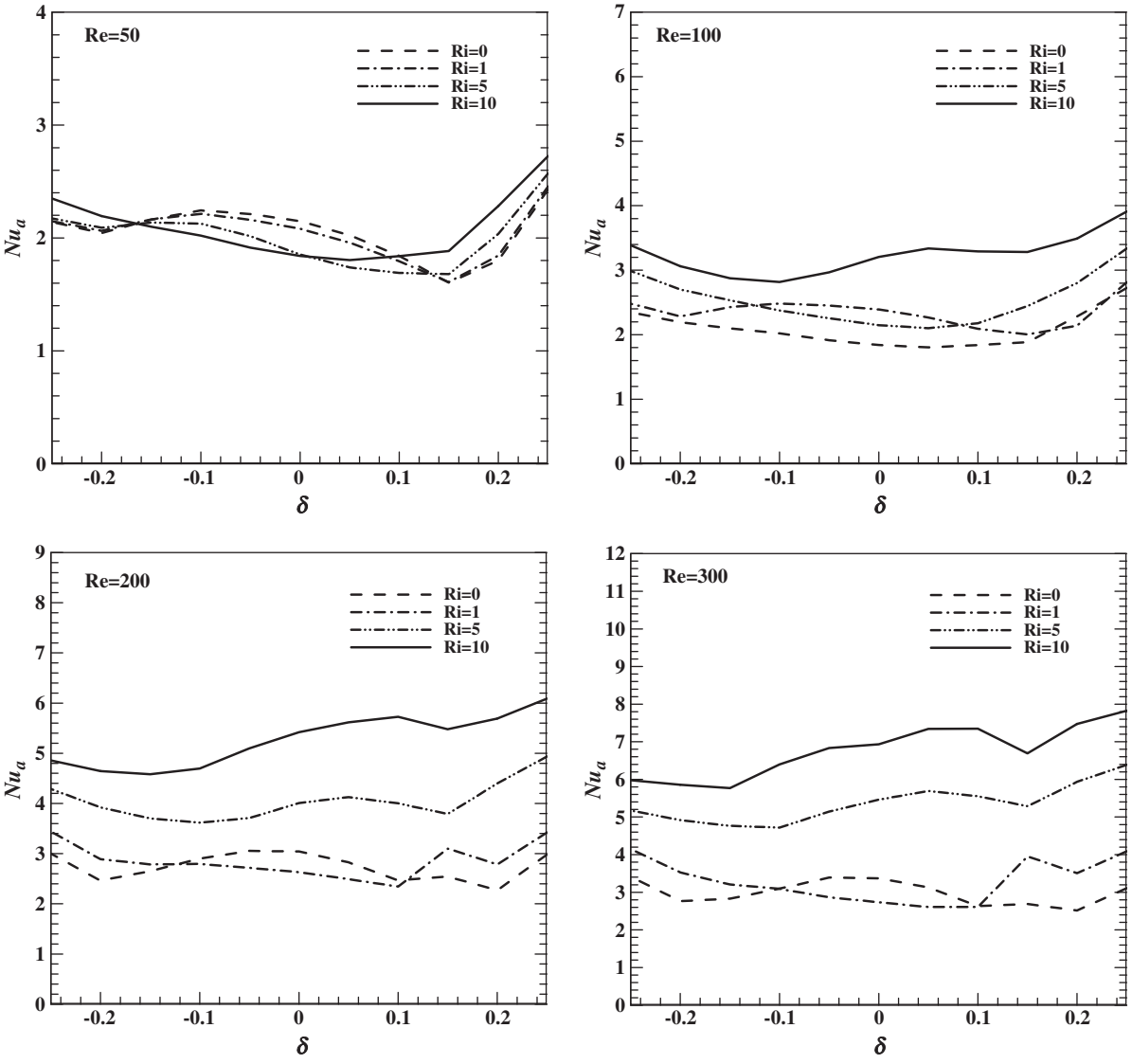

Fig. 8. Total surface-average Nusselt number of the enclosure hot left side wall along the δ for different Rayleigh and Reynolds numbers.

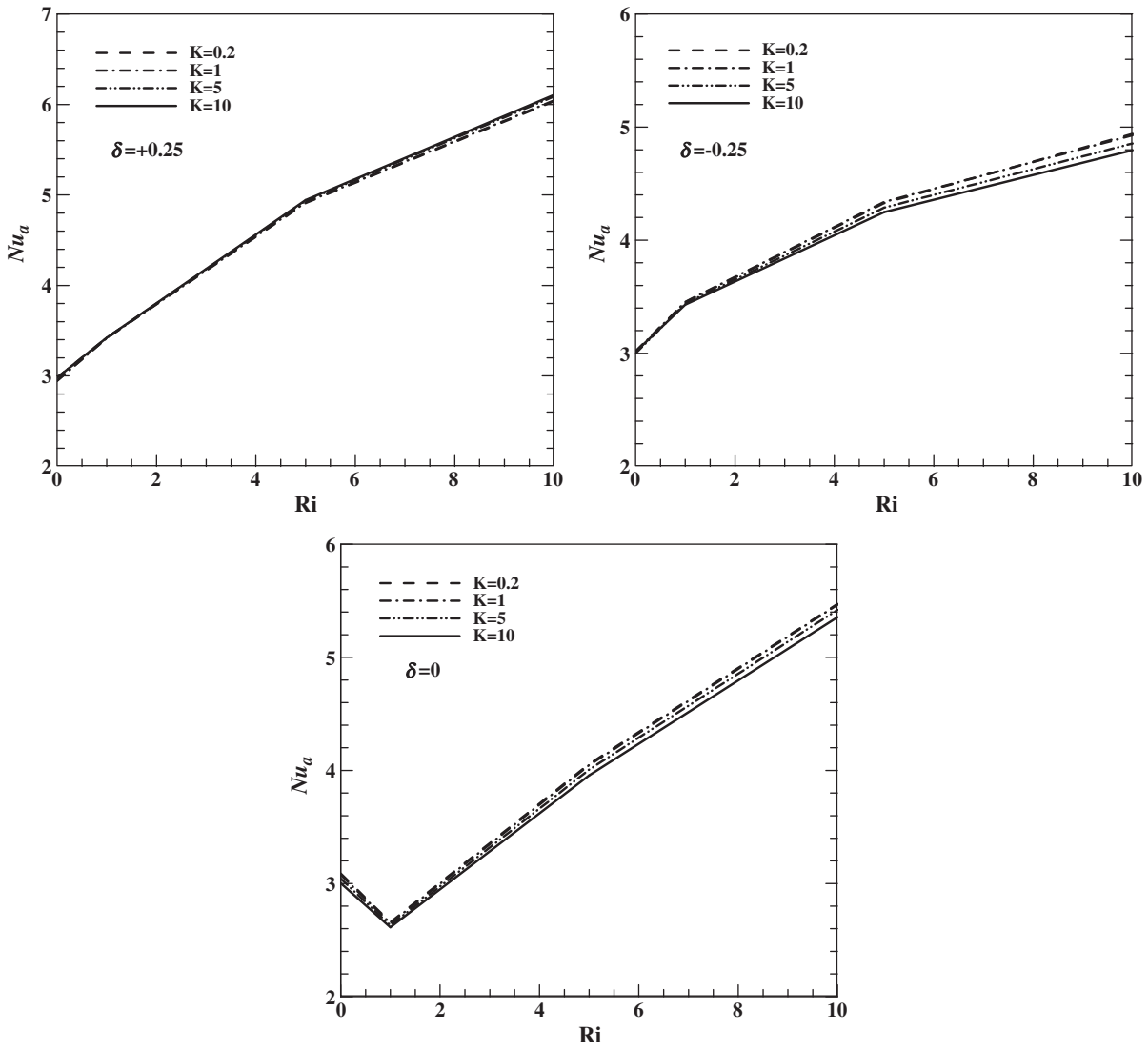

Fig. 9. Effect of solid–fluid thermal conductivity ratio on total surface-average Nusselt number of the enclosure hot left side wall for different values of δ and *Ri* while $Re = 200$.

reason of this phenomenon, since when the solid–fluid thermal conductivity ratio decreases, the thermal conductivity of rotating cylinder (k_s) becomes less than the thermal conductivity of the fluid (k) . This makes the rotating cylinder plays as an insulated material. From the other hand, the thermal conductivity of the fluid increases and added an additional amount of convection heat transfer causing to increase the average Nusselt number values.

7. Conclusions

The following conclusions can be drawn from the results of the present work:

1. When the Richardson number is small, major rotating vortices can be noticed around the rotating circular cylinder which is almost identical at $\delta = 0$. A very small minor vortices can be detected near the corners of the square enclosure, due to the domination of forced convection.
2. When the Richardson number is unity, no clear changes can be observed in the flow and thermal fields with the rotating circular cylinder locations (δ), since they are similar with the corresponding flow and thermal fields at the previous case when the Richardson number is $Ri = 0$.
3. Further increases in the Richardson number, cause the flow and thermal fields to be greatly affected. It is also observed that ,the minor vortices at the upper and lower edges of the square enclosure are increased in size, when the solid rotating circular cylinder moves upward in the domain $0 \le \delta \le +0.1$ or, when it moves downward in the domain $-0.1 \le \delta \le 0$.
4. When the Reynolds number increases, the circulation of flow vortices increases dramatically and becomes more stronger ,which leads to make the forced convection effect more dominant for different values of Richardson numbers and rotating circular cylinder locations (δ).
5. A thin thermal boundary layer can be observed clearly near the left hot side wall, when the Reynolds number increases.
6. It has been found that the solid–fluid thermal conductivity ratios (K) have a small effect on the flow field, since the streamlines are in general identical for all study cases.
7. It has been found that the solid–fluid thermal conductivity ratios (K) have a significant effect on the thermal field. Also the thermal boundary layers near the hot left side wall increases and concentrates as the solid–fluid thermal conductivity ratios (K) increases.
8. The results show that the average Nusselt number value increases as the Reynolds and Richardson numbers increase with selected upward and downward rotating circular cylinder locations.

9. No significant effect can be noticed of solid–fluid thermal conductivity ratios (K) on the average Nusselt number values. Also, at the hot left side wall of the enclosure when the solid–fluid thermal conductivity ratio decreases the average Nusselt number increases.

References

[1] K. Chang, H. Won, C. Cho, Patterns of natural convection around a square cylinder placed concentrically in a horizontal circular cylinder, ASME Journal of Heat Transfer 105, (1983) 273–280.

[2] E. Glakpe, A. Afsaw, Prediction of two-dimensional natural convection in enclosures with inner bodies of arbitrary shapes, Numerical Heat Transfer Part A 20, (1991) 279–296.

[3] A. Elepano, P. Oosthuizen, Free convective heat transfer from a heated cylinder in an enclosure with a cooled upper surface, Proceedings First International Conference-Advanced Computational Methods in Heat Transfer 2 (1990) 99–109.

[4] P. Oosthuizen, J. Paul, Free convective heat transfer from a heated half-cylinder in an enclosure, Proceedings CSME Forum, Montreal 1 (2) (1994) 365–378.

[5] W. Fu, C. Cheng, W. Shieh, Enhancement of natural convection heat transfer of an enclosure by a rotating circular cylinder, International Journal of Heat and Mass Transfer 37 (1994) 1885–1897.

[6] W. Fu, B.H. Tong, Numerical investigation of heat transfer from a heated oscillating cylinder in a cross flow, International Journal of Heat and Mass Transfer 45 (2002) 3033–3043.

[7] M. Ha, H. Yoon, K. Yoon, S. Balachandar, I. Kim, J. Lee, H. Chun, Two-dimensional and unsteady natural convection in a horizontal enclosure with a square body, Numerical Heat Transfer Part A 41 (2002) 183–198.

[8] M. Ha, I. Kim, H. Yoon, S. Lee, Unsteady fluid flow and temperature fields in a horizontal enclosure with an adiabatic body, Physics of Fluids 14 (2002) 3189–3207.

[9] D. Roychowdhury, S. Das, T. Sundararajan, Numerical simulation of natural convective heat transfer and fluid flow around a heated cylinder inside an enclosure, Heat and Mass Transfer 38 (2002) 565–576.

[10] A. De, A. Dalal, A numerical study of natural convection around a square, horizontal, heated cylinder placed in an enclosure, International Journal of Heat and Mass Transfer 49 (2006) 4608–4623.

[11] D. Angeli, P. Levoni, G. Barozzi, Numerical predictions for stable buoyant regimes within a square cavity containing a heated horizontal cylinder, International Journal of Heat and Mass Transfer 51 (2008) 553–565.

[12] J. Hwang, K. Yang, D. Yoon, K. Bremhorst, Flow field characterization of a rotating cylinder, International Journal of Heat and Fluid Flow 29 (2008) 1268–1278.

[13] M. Rahman, M. Alim, S. Saha, M. Chowdhury, A numerical study of mixed convection in a square cavity with a heat conducting square cylinder at different locations, Journal of Mechanical Engineering ME39 (2) (2008) 78–85.

[14] J. Ghazanfarian, M. Nobari, A numerical study of convective heat transfer from a rotating cylinder with cross-flow oscillation, International Journal of Heat and Mass Transfer 52 (2009) 5402–5411.

[15] Y. Shih, J. Khodadadi, K. Weng, A. Ahmed, Periodic fluid flow and heat transfer in a square cavity due to an insulated or isothermal rotating cylinder, ASME Journal of Heat Transfer 131 (2009) 1–11.

[16] H. Yoon, H. Chun, J. Kim, I. Ryong Park, Flow characteristics of two rotating side-by-side circular cylinder, Computers and Fluids 38 (2009) 466–474.

[17] S. Paramane, A. Sharma, Numerical investigation of heat and fluid flow across a rotating circular cylinder maintained at constant temperature in 2-D laminar flow regime, International Journal of Heat and Mass Transfer 52 (2009) 3205–3216.

[18] H. Oztop, Z. Zhao, B. Yub, Fluid flow due to combined convection in lid-driven enclosure having a circular body, International Journal of Heat and Fluid Flow 30 (2009) 886–901.

[19] M. Rahman, M. Alim, M. Mamun, Finite element analysis of mixed convection in a rectangular cavity with a heat-conducting horizontal circular cylinder, Non-linear Analysis: Modelling and Control 14 (2) (2009) 217–247.

[20] H. Yoon, M. Ha, B. Kim, D. Yu, Effect of the position of a circular cylinder in a square enclosure on natural convection at Rayleigh number of 10^7, Physics of Fluids 21 (2009) 21–31.

[21] V. Costa, A. Raimundo, Steady mixed convection in a differentially heated square enclosure with an active rotating circular cylinder, International Journal of Heat and Mass Transfer 53 (2010) 1208–1219.

[22] H. Mohammed, Y. Salman, Combined natural and forced convection heat transfer for assisting thermally developing flow in a uniformly heated vertical circular cylinder, International Communications in Heat and Mass Transfer 34 (2007) 474–491.

[23] G. Laskowski, S. Kearney, G. Evans, G. Greif, Mixed convection heat transfer to and from a horizontal cylinder in cross-flow with heating from below, International Journal of Heat and Fluid Flow 28 (2007) 454–468.

[24] J. Champigny, J. Simoneau, B. Duret, A les-experiment comparison of mixed convection around a large vertical cylinder, The 12th International Topical Meeting on Nuclear Reactor Thermal Hydraulics, Pittsburgh, Pennsylvania, U.S.A, 2007, pp. 1–21.

[25] S. Hussain, A. Hussein, Numerical investigation of natural convection phenomena in a uniformly heated circular cylinder immersed in square enclosure filled with air at different vertical locations, International Communications in Heat and Mass Transfer 37 (2010) 1115–1126.

[26] Saha, S., Hussein, A., Saha, G., Hussain, S. Mixed convection in a tilted lid-driven square enclosure with adiabatic cylinder at the center, International Journal of Heat and Technology, To be published.

[27] J. Ferzinger, M. Peric, Computational methods for fluid dynamics, Second EditionSpringer Verlag Publication, Berlin, 1999.

[28] H. Stone, Iterative solution of implicit approximations of multidimensional partial differential equations, SIAM Journal of Numerical Analysis 5 (1968) 530–558.

[29] S. Patankar, Numerical heat transfer and fluid flow, Hemisphere Publishing Corporation, New York, 1980.

[30] B. Kim, D. Lee, M. Ha, H. Yoon, A numerical study of natural convection in a square enclosure with a circular cylinder at different vertical locations, International Journal of Heat and Mass Transfer 51 (2008) 1888–1906.

[31] F. Moukalled, S. Acharya, Natural convection in the annulus between concentric horizontal circular and square cylinders, Journal of Thermophysics Heat Transfer 10 (1996) 524–531.